Biochemical and Biophysical Research Communications 452 (2014) 124–129

Contents lists available at ScienceDirect

Biochemical and Biophysical Research Communications

journal homepage: www.elsevier.com/locate/ybbrc

Crystal structure and biochemical characterization of PhaA from *Ralstonia eutropha*, a polyhydroxyalkanoate-producing bacterium

Eun-Jung Kim, Kyung-Jin Kim *

School of Life Sciences, KNU Creative BioResearch Group, Kyungpook National University, Daehak-ro 80, Buk-ku, Daegu 702-701, Republic of Korea

ARTICLE INFO

Article history:
Received 8 August 2014
Available online 21 August 2014

Keywords:
PhaA
Thiolase
Ralstonia eutropha
Crystal structure
Polyhydroxyalkanoates

ABSTRACT

PhaA from *Ralstonia eutropha* (*Re*PhaA) is the first enzyme in the polyhydroxyalbutyrate (PHB) biosynthetic pathway and catalyzes the condensation of two molecules of acetyl-CoA to acetoacetyl-CoA. To investigate the molecular mechanism underlying PHB biosynthesis, we determined the crystal structures of the *Re*PhaA protein in apo- and CoA-bound forms. The *Re*PhaA structure adopts the type II biosynthetic thiolase fold forming a tetramer by means of dimerization of two dimers. The crystal structure of *Re*PhaA in complex with CoA revealed that the enzyme contained a unique Phe219 residue, resulting that the ADP moiety binds in somewhat different position compared with that bound in other thiolase enzymes. Our study provides structural insight into the substrate specificity of *Re*PhaA. Results indicate the presence of a small pocket near the Cys88 covalent catalytic residue leading to the possibility of the enzyme to accommodate acetyl-CoA as a sole substrate instead of larger acyl-CoA molecules such as propionyl-CoA. Furthermore, the roles of key residues involved in substrate binding and enzyme catalysis were confirmed by site-directed mutagenesis.

1. Introduction

Over the past decade, efforts have been made to elucidate how to utilize the linear polyesters polyhydroxyalkanoates (PHAs) [1]. PHAs can be used to produce bioplastics, fine chemicals, implant biomaterials, pharmaceutical drugs, biofuels, and many others [2–5]. Although most petroleum-originated polymers are used on a wide scale today, the resources are being rapidly depleted and considered as non-sustainable materials. Hence, there is a strong need to develop alternatives. The PHA biosynthesis occurs in microorganisms grown in an aqueous solution, containing sustainable resources, such as, starch, glucose, sucrose, fatty acids, and nutrients in waste water at 30–37 °C and atmospheric pressure. Therefore, PHAs are considered sustainable, environmentally friendly plastics [6,7]. In order to store carbons as their energy source, bacteria produce PHAs via fermentation of either sugars or lipids [8]. Over 150 PHA monomers with different compositions, molecular weight, thermal and mechanical properties have been reported so far [9]. Considerable research has focused on understanding the mechanism of PHA biosynthesis and numerous advances have been made using molecular genetic analysis [10–12].

Biosynthetic production of PHAs generates polyesters with higher molecular weights than those produced by means of chemical methods. Moreover, various mechanisms of PHA production have been reported [9,13,14]. *Ralstonia eutropha* is the representative bacterial strain used for PHA biosynthesis, but several other bacteria, such as, *Aeromonas hydrophila*, *Pseudomonas stutzeri* [15], and *Pseudomonas oleovorans* have the same biosynthetic pathway to produce PHAs [12,16–19]. Three genes (*phaA*, *phaB*, and *phaC*) are involved in the PHA synthesis; *phaA* encodes β-ketothiolase, *phaB* encodes NADPH-dependent acetoacetyl-CoA reductase and *phaC* encodes PHA synthase [20].

The biosynthetic pathway of PHAs is divided into two consecutive stages, monomer synthesis and polymerization. Furthermore, genes originated from *R. eutropha* were engineered in *Escherichia coli* as well [21]. The synthesis of the (*R*)-3-hydroxybutyryl-CoA monomer involves two enzymes, PhaA and PhaB. First, PhaA catalyzes the condensation of two molecules of acetyl-CoA to acetoacetyl-CoA. Thereafter, acetoacetyl-CoA is converted to (*R*)-3-hydroxybutyryl-CoA by PhaB. PhaC catalyzes the polymerization step generating plastics. These plastics can be produced at 50% dry cell weight of the maximum theoretical yield [20]. Although the

* Corresponding author. Address: Structural and Molecular Biology Laboratory, School of Life Sciences and Biotechnology, Kyungpook National University, Daehak-ro 80, Buk-ku, Daegu 702-701, Republic of Korea. Fax: +82 53 955 5522.
E-mail address: kkim@knu.ac.kr (K.-J. Kim).

http://dx.doi.org/10.1016/j.bbrc.2014.08.074
0006-291X/

degradation reaction is stronger than the condensation reaction in PhaA, the PHA polymerization process is strongly driven by depletion of the PHA monomer by PhaC *in vivo*, which allows its physical sequestration as a polymer [5,22]. Therefore, PhaA and PhaB could sustain high rate of PHA production if a similar irreversible physical step took place later in the reaction, such as the release of free CoAs or secretion of the *n*-butanol product from the cell [23].

Given the potential role of PHAs as a bioplastics, the ultimate goal is to improve the efficiency of each step of their biosynthesis, while developing enzymes that can produce other types of valuable copolymers. Recently, our group determined the crystal structure of PhaB from *R. eutropha* and elucidated the molecular mechanism of the conversion of acetoacetyl-CoA to (*R*)-3-hydroxybutyryl-CoA [24]. PhaA is the first enzyme in the PHA biosynthesis pathway and determines the carbon composition of the PHA monomers. Therefore, structural information of PhaA could provide key details to improve its efficiency at the molecular level. In this study, we report the crystal structure of PhaA from *R. eutropha* H16, as an apo-enzyme and in complex with a substrate. Additionally, we provide structural insights into the substrate binding mode and substrate specificity.

2. Materials and methods

2.1. Preparation of RePhaA

Cloning, expression, purification, and crystallization of *Re*PhaA will be described elsewhere (Kim et al., in preparation). Briefly, the *Re*PhaA coding gene (Met1–Lys393, 40.5 kDa) was amplified by polymerase chain reaction (PCR) using *R. eutropha* chromosomal DNA as a template. The PCR product was then subcloned into pProEX HTa (Life Technology) with a 6×-histag and rTEV protease cleavage site at the N-terminus. The expression construct was transformed into an *E. coli* BL21 (DE3) strain, which was grown in 1 L of LB medium containing ampicilin (50 mg/mL) at 37 °C. After induction via the addition of 1.0 mM IPTG, the culture medium was further maintained for 20 h at 18 °C. The culture was harvested by centrifugation at 5000*g* at 4 °C. The cell pellet was resuspended in buffer A (40 mM Tris–HCl at pH 8.0 and 5 mM β-mercaptoethanol) and then disrupted by ultrasonication. The cell debris was removed by centrifugation at 11,000*g* for 1 h, and lysate was bound to Ni–NTA agarose (QIAGEN). After washing with buffer A containing 20 mM imidazole, the bound proteins were eluted with 300 mM imidazole in buffer A. The 6×-histag was removed from the *Re*PhaA protein by incubating with rTEV protease (GIBCO). A trace amount of contamination was removed by applying HiLoad 26/60 Superdex 200 prep grade (GE Healthcare) size exclusion chromatography. The purified protein showed ~95% purity on SDS–PAGE, was concentrated to 25 mg/mL in 40 mM Tris–HCl, pH 8.0, 1 mM dithiothreitol. For the production of *Re*PhaA mutant proteins, site-directed mutagenesis experiments were performed and the mutant proteins were purified with a procedure similar to that of the wild-type *Re*PhaA.

2.2. Crystallization and data collection of RePhaA

Suitable crystals for diffraction experiments were obtained at 22 °C within 7 days from the precipitant of 20% polyethylene glycol monomethyl ether (PEGMME) 2 K, 0.1 M Tris–HCl pH 8.5 and 0.2 M trimethylamine N-oxide dihydrate. The crystals were transferred to cryoprotectant solution containing 20% polyethylene glycol monomethyl ether (PEGMME) 2 K, 0.1 M Tris–HCl pH 8.5, 0.2 M trimethylamine N-oxide dihydrate and 20% (v/v) glycerol, fished out with a loop larger than the crystals and flash-frozen by immersion in liquid nitrogen at −173 °C. The data were collected to a resolution of 1.96 Å at 7A beamline of the Pohang Accelerator Laboratory (PAL, Pohang, Korea) using a Quantum 270 CCD detector (ADSC, USA). The data were then indexed, integrated, and scaled using the HKL2000 suite [25]. Crystals of an apo-form belonged to space group $P2_1$, with unit cell parameters of $a = 63.377$ Å, $b = 105.474$ Å, $c = 106.914$ Å, $\alpha = \gamma = 90°$ and $\beta = 106.176°$. Assuming four molecules of *Re*PhaA per asymmetric unit, the crystal volume per unit of protein mass was 2.29 $Å^3\ Da^{-1}$, which corresponds to a solvent content of approximately 46.22% [26]. *Re*PhaA crystals in complex with CoA were crystallized with the crystallization condition of 25% PEG3350, 0.1 M HEPES pH 7.5 and 0.2 M ammonium sulfate, supplemented with 25 mM of CoA. Crystals in complex with CoA belonged to $P2_1$, with unit cell parameters of $a = 102.092$ Å, $b = 157.438$ Å, $c = 114.867$ Å, $\alpha = \gamma = 90°$ and $\beta = 90.004°$. Assuming eight molecules of *Re*PhaA per asymmetric unit, the crystal volume per unit of protein mass was 2.85 $Å^3\ Da^{-1}$, which corresponds to a solvent content of approximately 56.86% [26].

2.3. Structure determination of RePhaA

The structure was determined by molecular replacement with the CCP4 version of MOLREP [27] using the structure of beta-keto thiolase B from *R. eutropha* (*Re*BktB) (PDB code 4NZS) as a search model. The Model building was performed manually using the program WinCoot [28] and the refinement was performed with CCP4 refmac5 [29] and CNS [30]. The *Re*PhaA structure in complex with CoA was determined by molecular replacement with the CCP4 version of MOLREP using the apo-form of *Re*PhaA structure as a search model. Model building and structure refinement of the *Re*PhaA structure in complex with CoA were similarly performed with

Table 1
Data collection and refinement statistics.

	*Re*PhaA	
	APO	C88S_With coenzyme A
Data collection		
Space group	$P2_1$	$P2_1$
Cell dimensions		
a, *b*, *c* (Å)	63.377, 105.474, 106.914	102.092, 157.438, 114.867
α, β, γ (°)	90.00, 106.176, 90.00	90.00, 90.004, 90.00
Resolution (Å)	50.00–1.96 (1.99–1.96)*	50.00–2.0 (2.03–2.0)
R_{sym} or R_{merge}	12.8 (25.4)	6.8 (15.6)
$I/\sigma I$	48.15 (19.97)	48.24 (19.05)
Completeness (%)	94.9 (98.3)	98.6 (98.1)
Redundancy	6.7 (5.8)	7.4 (7.3)
Refinement		
Resolution (Å)	30.00–1.96	27.71–2.00
No. reflections	93,153	226,361
R_{work}/R_{free}	17.1 / 23	17.3 / 21.3
No. atoms	12,325	23,988
Protein	11,307	22,687
Ligand/ion	12	48
Water	1006	922
B-factors	22.474	23.324
Protein	21.953	22.395
Ligand/ion	29.197	110.551
Water	31.094	22.076
R.m.s. deviations		
Bond lengths (Å)	0.018	0.019
Bond angles (°)	1.817	2.038

AU: equations defining various *R*-values are standard and hence are no longer defined in the footnotes.
[AU: Ramachandran statistics should be in Methods section at the end of Refinement subsection.
[AU: wavelength of data collection, temperature and beamline should all be in Methods section.
* Number of xtals for each structure should be noted in footnote. Values in parentheses are for highest-resolution shell.

those of the apo-form of *Re*PhaA. The refined models of the apo- and the CoA-bound forms of *Re*PhaA were deposited to protein data bank with pdb codes of 4O99 and 4O9C, respectively. The data statistics are summarized in Table 1.

2.4. Thiolase activity assay

The reaction mixture (a total volume 1 mL) contained 100 mM Tris–HCl pH 8.0, 10 mM of $MgCl_2$, 50 μM of CoA, 50 μM acetoacetyl CoA and *Re*PhaA (5 μM). After pre-incubation at 30 °C for 5 min, the reaction was initiated by the addition of enzyme. And the decrease of acetoacetyl-CoA was measured by monitoring decrease of absorbance at 303 nm using an extinction coefficient of 14×10^3.

3. Results and discussion

3.1. Overall structure of RePhaA

In order to elucidate the enzymatic properties of the *Re*PhaA protein, we determined its crystal structure at 1.96 Å resolution (Fig. 1). The asymmetric unit of the crystal contained four *Re*PhaA molecules, which corresponded to a tetrameric structure of *Re*PhaA. Further, size-exclusion chromatography results suggested that the protein exists as a tetramer (data not shown). In order to

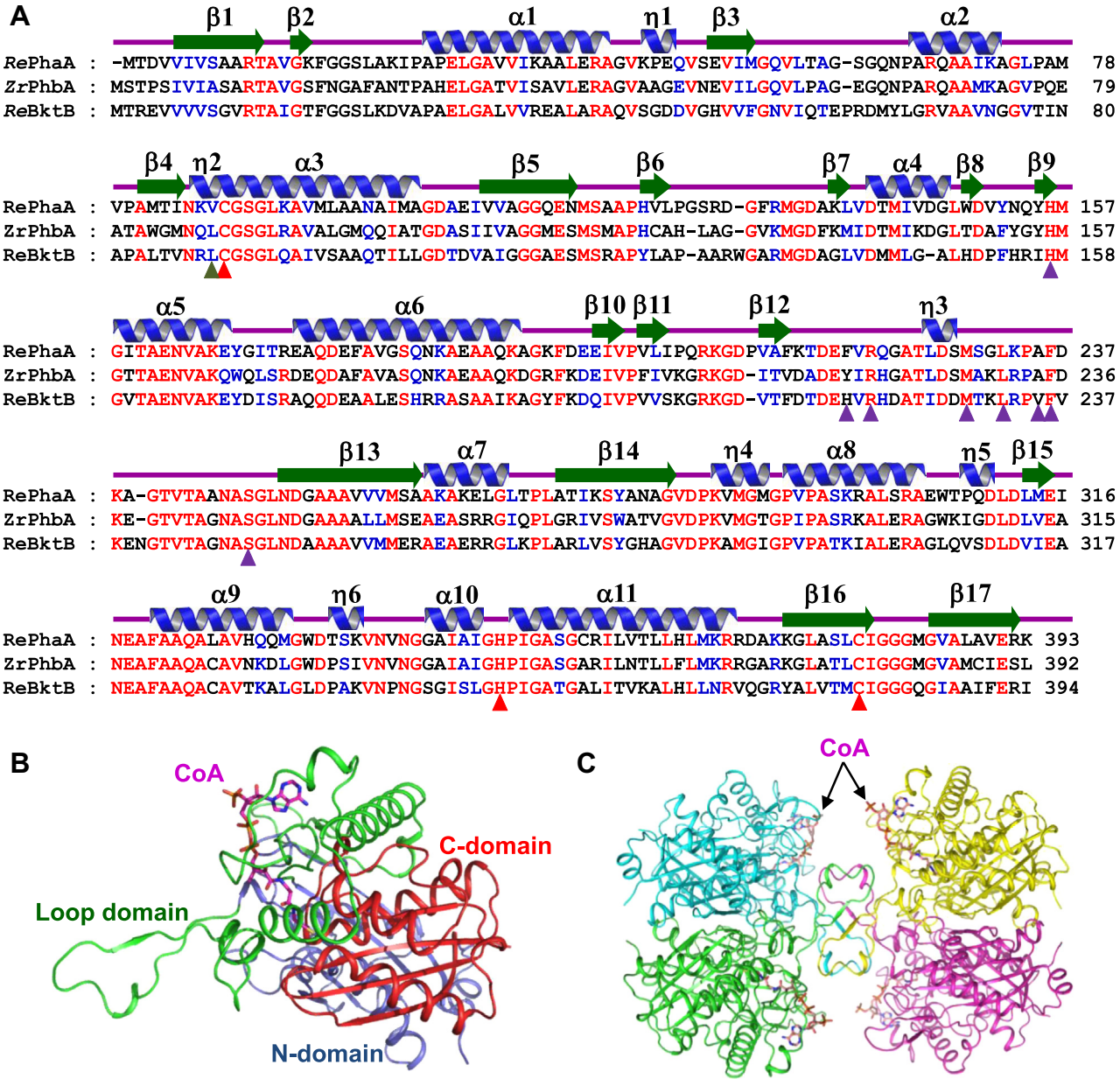

Fig. 1. Overall shape of *Re*PhaA. (A) Amino acid sequence alignment of thiolases. Secondary structure elements are shown based on the *Re*PhaA structure. Identical and highly conserved residues are presented in red and blue colored characters, respectively. Residues involved in the enzyme catalysis, substrate binding and substrate specificity are marked with red-, purple-and green-colored rectangles, respectively. (B) Overall shape of *Re*PhaA monomer. The *Re*PhaA monomer is presented with a cartoon diagram. The N-terminal, C-terminal and Loop domains are distinguished with light-blue, red and green colors, respectively. The bound-CoA is shown with a stick model with magenta color. (C) Overall shape of *Re*PhaA tetramer. Four polypeptides are differentiated by colors of cyan, green, yellow and magenta. The bound-CoA is shown with a stick model with magenta color. Four CoA molecules bound in the each four polypeptides are shown with a stick model with magenta color. (For interpretation of the references to color in this figure legend, the reader is referred to the web version of this article.)

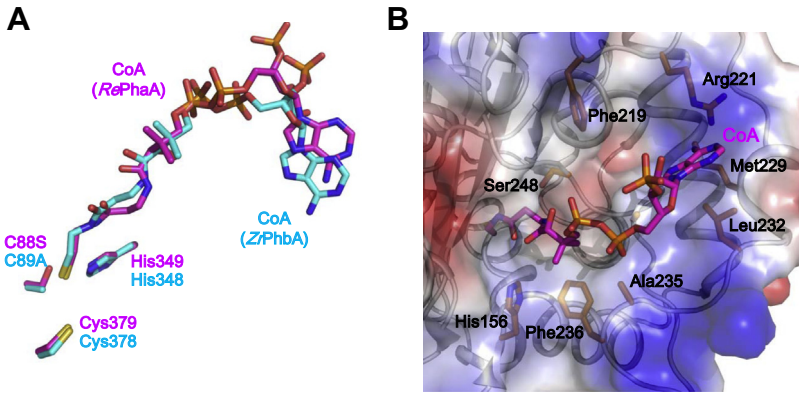

Fig. 2. Substrate binding mode of *Re*PhaA. (A) Difference in positions of bound CoAs in *Re*PhaA and *Zr*PhbA. CoA-bound forms of *Re*BktB and *Zr*PhbA are superposed and the bound-CoAs are shown with stick models and labeled appropriately. Three catalytic residues of *Re*BktB and *Zr*PhbA are shown with stick models and labeled appropriately. (B) Substrate binding pocket of *Re*PhaA. The *Re*PhaA structure is presented with both a cartoon and an electrostatic surface potential model. The residues involved in the substrate binding are shown as a stick model with orange color and labeled. The bound-CoA is shown as a stick model with magenta color. (For interpretation of the references to color in this figure legend, the reader is referred to the web version of this article.)

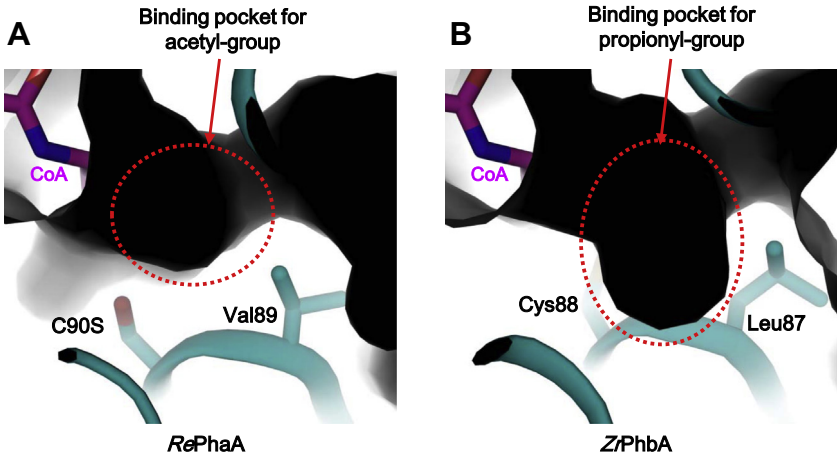

Fig. 3. Substrate binding specificity of *Re*PhaA and *Re*BktB. The binding pocket for acetyl- or propionyl-group that is covalently bonded at the first step of thiolase reaction, is presented. The structures of *Re*PhaA (A) and *Re*BktB (B) are presented with cartoon diagrams with cyan color. And the structures are presented with electrostatic surface potential models as well to show the binding pocket for acetyl- or propionyl-group. The binding pocket for acetyl-group in *Re*PhaA (A) and that for propionyl-group in *Re*BktB (B) are marked with dotted-circles and labeled appropriately. The bound CoAs are shown as stick models with magenta color. The residues determining the substrate specificity and the covalent catalytic cysteine residues are shown as stick models and labeled. (For interpretation of the references to color in this figure legend, the reader is referred to the web version of this article.)

define the substrate binding mode of *Re*PhaA, we also determined the crystal structure of the enzyme in complex with coenzyme A (CoA) at 2.0 Å resolution. The CoA-bound form of the crystal contained eight molecules, which corresponded to two functional *Re*PhaA tetramers. The atomic structures had good agreement with the X-ray crystallographic statistics of bond angles, bond lengths, and other geometric parameters (Table 1).

The overall structure of *Re*PhaA was similar to that of the type II biosynthetic thiolases, such as the PhbA thiolase from *Zoogloea ramigera* (*Zr*PhbA) [31] and beta-keto thiolase B from *R. eutropha* (*Re*BktB) [32]. Considering that *Re*PhaA catalyzes the first reaction of the PHB synthesis by condensing two acetyl-CoA molecules, the enzyme adopts the type II biosynthetic thiolase fold. The structure of *Re*PhaA consisted of two distinctive domains, a core and a loop domain. The core domain was divided into N-terminal (residues 1–117 and 252–272) and C-terminal (residues 273–393) core domains, and the loop domain was located between the two core domains (L-domain, residues 118–251) (Fig. 1B). The N- and C-domains contained an α-β-α-β-α structure with a mixture of α-helices and β-sheets, which is a typical topology for the thiolase family enzymes. In the N-domain, six β-sheets were packed and covered by four α-helixes. The C-domain was also composed of four β-sheets packed evenly, and four α-helices covered the β-sheets. The L-domain consisted of four α-helices and three short β-sheets, forming a triangular shape. This domain also contained a sequence motif (residues 123–142) involved in the tetramerization of the protein (Fig. 1B). The tetramer structure of *Re*PhaA was formed by contact only between the L-loop domains of the four polypeptides (Fig. 1C).

3.2. Catalytic site of RePhaA

It has been reported that type II biosynthetic thiolase uses two cysteine residues for enzyme catalysis. In *Zr*PhbA, the residues of Cys89 and Cys378 function as a covalent catalyst and a second nucleophile, respectively [31]. In our *Re*PhaA structure, two cysteine residues, Cys88 and Cys379, were observed to be located at similar positions corresponding to Cys89 and Cys378 residues in *Zr*PhbA. The Cys90 residue was located at the connecting loop between β3 and α3 of the N-domain, and the Cys380 residue was at the β12 of the C-domain (Fig. 2A). Furthermore, the His349 residue was located near the Cys88 residue, and appeared to function as a general base. The superposition of *Re*PhaA and *Zr*PhbA structures also revealed that the His348 residue in *Zr*PhbA was located

at a position similar to that of the His349 residue in *Re*PhaA (Fig. 2A). The role of the three residues, Cys88, Cys379, and His349, in the *Re*PhaA catalysis was further confirmed by site-directed mutagenesis experiments. All the three mutants, C88S, C379S, and H349A, exhibited almost a complete loss of activity, suggesting that *Re*PhaA has a catalytic mechanism similar to that of other type II biosynthetic thiolases, such as, *Zr*PhbA and *Re*BktB (See Fig. 4).

3.3. Substrate binding mode of RePhaA

The substrate binding mode of *Re*PhaA was elucidated using the crystal structure of C88S mutant in complex with CoA. The overall structure of the CoA-bound structure was almost identical to that of the apo-form of the enzyme. Overall, *Re*PhaA adopts a unique binding mode of ADP moiety compared with that of *Zr*PhbA, whereas the binding modes of the β-mercaptoethylamine and pantothenic acid moieties of CoA are quite similar to each other. In *Zr*PhbA, the Ser247 and His156 residues were involved in the stabilization of the β-mercaptoethylamine and pantothenic acid moieties of CoA. Ser248 and His156 residues were also found in *Re*PhaA at positions similar to that of the corresponding residues in *Zr*PhbA (Fig. 2B). Further, site-directed mutagenesis experiments confirmed the involvement of these two residues in the stabilization of the β-mercaptoethylamine and pantothenic acid moieties. The S248A and H156A *Re*PhaA mutants showed reduced or complete loss of enzyme activity, respectively (Fig. 4). The ADP moiety was found to be bound in a hydrophobic pocket in *Re*PhaA constituted by residues of Met229, Leu232, Ala235, Phe236, and Ala244; the same can be also found in *Zr*PhbA. One exceptional difference is that the Phe219 residue in *Re*PhaA provides marked hydrophobicity for the binding of ADP moiety, whereas the corresponding Tyr218 residue posseses water-mediated hydrogen bond with the phosphate moiety in *Zr*PhbA (Fig. 2B). The marked hydrophobicity of the residue led to a position difference of the bound-ADP moiety between these two enzymes. In fact, the bound-ADP moiety in *Re*PhaA was located more toward the solvent area than the moiety in *Zr*PhbA (Fig. 2A). In order to verify the function of the Phe219 residue, we generated two mutants, F219A and F219Y. Interestingly, the F219Y mutant showed more than 2-fold activity, whereas the F219A mutant evidenced approximately 30% activity compared with the wild-type *Re*PhaA (Fig. 4). This result indicates that the bulky amino acid at the position of Phe219 is important for the stabilization of the ADP moiety, providing van der Waals interaction with the moiety. However, the water-mediated hydrogen bond between the tyrosine residue and the pyrophosphate moiety might enable a tighter binding of the substrate to the enzyme, thus leading to higher enzyme activity.

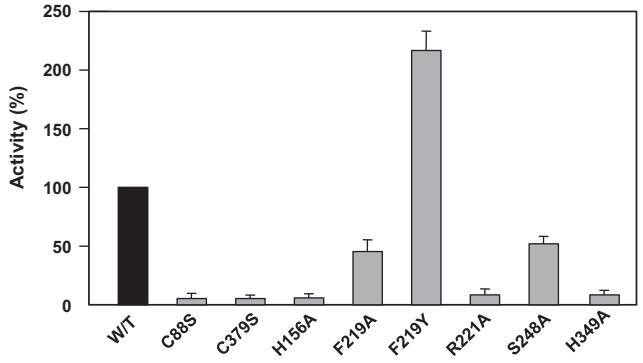

Fig. 4. Site-detected mutagenesis of *Re*PhaA. Residues involved in enzyme catalysis (Cys88, Cys379, and His156) and substrate binding (Phe219, Arg221, Ser248, and His349) were replaced by appropriate residues. The relative activities of recombinant mutant proteins were measured and compared with that of wild-type *Re*PhaA.

3.4. Substrate specificity of thiolases

R. eutropha chromosome contains two type II biosynthetic thiolases, *Re*PhaA and *Re*BktB. They are involved in the synthesis of PHAs. Moreover, the *Re*BktB coding gene is located approximately 4 kilobases downstream of the *pha* operon (*phaA*, *phaB*, and *phaC*) [33]. Although *Re*PhaA is solely involved in the production of PHB by catalyzing the condensation reaction of two acetyl-CoA molecules, *Re*BktB is known to be involved in the production of PHB and polyhydroxybutyratehydroxyvalerate copolymer (PHBHV); the latter is produced by condensing acetyl-CoA and propionyl-CoA [4]. This difference in substrate specificity can be explained by comparing the structures of these two thiolases, while taking into consideration the catalytic mechanism of thiolase. The first step of thiolase reaction is the Cys88 thiol-group nucleophilic attack on the first substrate, acetyl-CoA or propionyl-CoA, that leads to the formation of the thioester bond between Cys88 and the acetyl- or propionyl-group. During the second step, the nucleophilic Cys378 attacks the acetylated or propionylated thioester bond of Cys88, leading to the condensation of acetyl- or propionyl-group from the first substrate to the second substrate acetyl-CoA. It can be assumed that *Re*BktB might require a larger space to accommodate covalently bonded propionyl-group compared to *Re*PhaA, which only accommodates covalently bonded acetyl-group. After detailed structural comparison, we observed a striking difference between these two thiolases regarding the binding pocket of covalently bonded acetyl- or propionyl-group. The Val87 residue was located near the Cys88 covalent catalytic residue in *Re*PhaA, while the corresponding Leu88 residue was located near the Cys90 covalent catalytic residue in *Re*BktB. The difference resulted in a larger space near the covalent catalytic residue in *Re*BktB, which might enable the enzyme to catalyze the condensation of both acetyl- and propionyl-CoA to acetyl-CoA (Fig. 3).

Acknowledgments

This work was supported by the National Research Foundation of Korea (NRF) Grant funded by the Korean Government (MEST) (NRF-2009-C1AAA001-2009-0093483, and NRF-2014M1A2A2033626) and by the Advanced Biomass R&D Center (ABC) of Global Frontier Project funded by the MEST (ABC-2012-053895).

References

[1] G.Q. Chen, A microbial polyhydroxyalkanoates (PHA) based bio- and materials industry, Chem. Soc. Rev. 38 (2009) 2434–2446.
[2] J. Jian, S.Q. Zhang, Z.Y. Shi, W. Wang, G.Q. Chen, Q. Wu, Production of polyhydroxyalkanoates by *Escherichia coli* mutants with defected mixed acid fermentation pathways, Appl. Microbiol. Biotechnol. 87 (2010) 2247–2256.
[3] T. Keshavarz, I. Roy, Polyhydroxyalkanoates: bioplastics with a green agenda, Curr. Opin. Microbiol. 13 (2010) 321–326.
[4] X. Gao, J.C. Chen, Q. Wu, G.Q. Chen, Polyhydroxyalkanoates as a source of chemicals, polymers, and biofuels, Curr. Opin. Biotechnol. 22 (2011) 768–774.
[5] L. Mauclaire, E. Brombacher, J.D. Bunger, M. Zinn, Factors controlling bacterial attachment and biofilm formation on medium-chain-length polyhydroxyalkanoates (mcl-PHAs), Coll. Surf. B Biointerf. 76 (2010) 104–111.
[6] S.Y. Lee, J.I. Choi, Production and degradation of polyhydroxyalkanoates in waste environment, Waste Manage. 19 (1999) 133–139.
[7] H. Ariffin, H. Nishida, M.A. Hassan, Y. Shirai, Chemical recycling of polyhydroxyalkanoates as a method towards sustainable development, Biotechnol. J. 5 (2010) 484–492.
[8] K. Sudesh, H. Abe, Y. Doi, Synthesis, structure and properties of polyhydroxyalkanoates: biological polyesters, Prog. Polym. Sci. 25 (2000) 1503–1555.
[9] W.N. He, Z.M. Zhang, P. Hu, C.Q. Chen, Microbial synthesis and characterization of polyhydroxyalkanoates by DG17 from glucose, Acta Polym. Sin. (1999) 709–714.

[10] A.J. Anderson, E.A. Dawes, Occurrence, metabolism, metabolic role, and industrial uses of bacterial polyhydroxyalkanoates, Microbiol. Rev. 54 (1990) 450–472.
[11] A. Steinbuchel, E. Hustede, M. Liebergesell, U. Pieper, A. Timm, H. Valentin, Molecular-basis for biosynthesis and accumulation of polyhydroxyalkanoic acids in bacteria, FEMS Microbiol. Lett. 103 (1992) 217–230.
[12] X. Gao, J. Jian, W.J. Li, Y.C. Yang, X.W. Shen, Z.R. Sun, Q. Wu, G.Q. Chen, Genomic study of polyhydroxyalkanoates producing *Aeromonas hydrophila* 4AK4, Appl. Microbiol. Biotechnol. 97 (2013) 9099–9109.
[13] J.E. Kemnitzer, S.P. Mccarthy, R.A. Gross, Preparation of predominantly syndiotactic poly(beta-hydroxybutyrate) by the tributyltin methoxide catalyzed ring-opening polymerization of racemic beta-butyrolactone, Macromolecules 26 (1993) 1221–1229.
[14] E.N. Pederson, C.W.J. McChalicher, F. Srienc, Bacterial synthesis of PHA block copolymers, Biomacromolecules 7 (2006) 1904–1911.
[15] S. Ciesielski, J. Mozejko, G. Przybylek, The influence of nitrogen limitation on mcl-PHA synthesis by two newly isolated strains of *Pseudomonas* sp, J. Ind. Microbiol. Biotechnol. 37 (2010) 511–520.
[16] X.R. Han, Y. Satoh, T. Satoh, K. Matsumoto, T. Kakuchi, S. Taguchi, T. Dairi, M. Munekata, K. Tajima, Chemo-enzymatic synthesis of polyhydroxyalkanoate (PHA) incorporating 2-hydroxybutyrate by wild-type class I PHA synthase from *Ralstonia eutropha*, Appl. Microbiol. Biotechnol. 92 (2011) 509–517.
[17] T. Kichise, T. Fukui, Y. Yoshida, Y. Doi, Biosynthesis of polyhydroxyalkanoates (PHA) by recombinant *Ralstonia eutropha* and effects of PHA synthase activity on in vivo PHA biosynthesis, Int. J. Biol. Macromol. 25 (1999) 69–77.
[18] A. Pohlmann, W.F. Fricke, F. Reinecke, B. Kusian, H. Liesegang, R. Cramm, T. Eitinger, C. Ewering, M. Potter, E. Schwartz, A. Strittmatter, I. Voss, G. Gottschalk, A. Steinbuchel, B. Friedrich, B. Bowien, Genome sequence of the bioplastic-producing "Knallgas" bacterium *Ralstonia eutropha* H16, Nat. Biotechnol. 24 (2006) 1257–1262.
[19] B. Fuchtenbusch, A. Steinbuchel, Biosynthesis of polyhydroxyalkanoates from low-rank coal liquefaction products by *Pseudomonas oleovorans* and *Rhodococcus ruber*, Appl. Microbiol. Biotechnol. 52 (1999) 91–95.
[20] O.P. Peoples, A.J. Sinskey, Poly-beta-hydroxybutyrate (Phb) biosynthesis in alcaligenes-eutrophus H16 – identification and characterization of the Phb polymerase gene (Phbc), J. Biol. Chem. 264 (1989) 15298–15303.
[21] M. Shiraki, T. Endo, T. Saito, Fermentative production of (*R*)-(−)-3-hydroxybutyrate using 3-hydroxybutyrate dehydrogenase null mutant of Ralstonia eutropha and recombinant *Escherichia coli*, J. Biosci. Bioeng. 102 (2006) 529–534.
[22] T. Kichise, S. Taguchi, Y. Doi, Enhanced accumulation and changed monomer composition in polyhydroxyalkanoate (PHA) copolyester by in vitro evolution of *Aeromonas caviae* PHA synthase, Appl. Environ. Microbiol. 68 (2002) 2411–2419.
[23] B. Bowien, B. Kusian, Genetics and control of CO_2 assimilation in the chemoautotroph *Ralstonia eutropha*, Arch. Microbiol. 178 (2002) 85–93.
[24] J. Kim, J.H. Chang, E.J. Kim, K.J. Kim, Crystal structure of (*R*)-3-hydroxybutyryl-CoA dehydrogenase PhaB from *Ralstonia eutropha*, Biochem. Biophys. Res. Commun. 443 (2014) 783–788.
[25] Z. Otwinowski, W. Minor, Processing of X-ray diffraction data collected in oscillation mode, Macromol. Crystallogr. Pt. A 276 (1997) 307–326.
[26] B.W. Matthews, Solvent content of protein crystals, J. Mol. Biol. 33 (1968) 491–497.
[27] A. Vagin, A. Teplyakov, Molecular replacement with MOLREP, Acta Crystallogr. D Biol. Crystallogr. 66 (2010) 22–25.
[28] P. Emsley, K. Cowtan, Coot: model-building tools for molecular graphics, Acta Crystallogr. D Biol. Crystallogr. 60 (2004) 2126–2132.
[29] G.N. Murshudov, A.A. Vagin, E.J. Dodson, Refinement of macromolecular structures by the maximum-likelihood method, Acta Crystallogr. D Biol. Crystallogr. 53 (1997) 240–255.
[30] A.T. Brunger, P.D. Adams, G.M. Clore, W.L. DeLano, P. Gros, R.W. Grosse-Kunstleve, J.S. Jiang, J. Kuszewski, M. Nilges, N.S. Pannu, R.J. Read, L.M. Rice, T. Simonson, G.L. Warren, Crystallography & NMR system: a new software suite for macromolecular structure determination, Acta Crystallogr. D Biol. Crystallogr. 54 (1998) 905–921.
[31] Y. Modis, R.K. Wierenga, Crystallographic analysis of the reaction pathway of *Zoogloea ramigera* biosynthetic thiolase, J. Mol. Biol. 297 (2000) 1171–1182.
[32] E.J. Kim, H.F. Son, S. Kim, J.W. Ahn, K.J. Kim, Crystal structure and biochemical characterization of beta-keto thiolase B from polyhydroxyalkanoate-producing bacterium *Ralstonia eutropha* H16, Biochem. Biophys. Res. Commun. 444 (2014) 365–369.
[33] S. Slater, K.L. Houmiel, M. Tran, T.A. Mitsky, N.B. Taylor, S.R. Padgette, K.J. Gruys, Multiple beta-ketothiolases mediate poly(beta-hydroxyalkanoate) copolymer synthesis in *Ralstonia eutropha*, J. Bacteriol. 180 (1998) 1979–1987.